PHYSICAL REVIEW E **94**, 011201(R) (2016)

Core conditions for alpha heating attained in direct-drive inertial confinement fusion

A. Bose,[1,2] K. M. Woo,[1,2] R. Betti,[1,2] E. M. Campbell,[2] D. Mangino,[2] A. R. Christopherson,[1,2] R. L. McCrory,[2] R. Nora,[3] S. P. Regan,[2] V. N. Goncharov,[2] T. C. Sangster,[2] C. J. Forrest,[2] J. Frenje,[4] M. Gatu Johnson,[4] V. Yu Glebov,[2] J. P. Knauer,[2] F. J. Marshall,[2] C. Stoeckl,[2] and W. Theobald[1,2]

[1]*Fusion Science Center, University of Rochester, Rochester, New York 14623, USA*

[2]*Laboratory for Laser Energetics, University of Rochester, Rochester New York 14623, USA*

[3]*Lawrence Livermore National Laboratory, Livermore, California 94550, USA*

[4]*Massachusetts Institute of Technology, Plasma Science and Fusion Center, Cambridge, Massachusetts 02139, USA*

(Received 16 December 2015; published 7 July 2016)

It is shown that direct-drive implosions on the OMEGA laser have achieved core conditions that would lead to significant alpha heating at incident energies available on the National Ignition Facility (NIF) scale. The extrapolation of the experimental results from OMEGA to NIF energy assumes only that the implosion hydrodynamic efficiency is unchanged at higher energies. This approach is independent of the uncertainties in the physical mechanism that degrade implosions on OMEGA, and relies solely on a volumetric scaling of the experimentally observed core conditions. It is estimated that the current best-performing OMEGA implosion [Regan *et al.*, Phys. Rev. Lett. **117**, 025001 (2016)] extrapolated to a 1.9 MJ laser driver with the same illumination configuration and laser-target coupling would produce 125 kJ of fusion energy with similar levels of alpha heating observed in current highest performing indirect-drive NIF implosions.

DOI: 10.1103/PhysRevE.94.011201

Inertial confinement fusion (ICF) [1] uses lasers or other drivers such as pulsed-power devices or particle accelerators to implode a shell of cryogenic deuterium and tritium (DT). Laser light can be directly incident on the capsule surface (direct drive) or converted into x-rays (indirect drive) through a high-Z enclosure (hohlraum). The shell is imploded to high velocities of hundreds km/s to achieve high central temperatures and areal densities [2]. The hot spot (∼5–10 keV) is a low-density (30–100 g/cm^3) core and is surrounded and tamped by a cold (200–500 eV) near Fermi-degenerate dense (300–1000 g/cm^3) fuel layer. Fusion alphas produced in the hot spot deposit their energy primarily through collisions with plasma electrons further enhancing the temperature and fusion reaction rate (alpha heating). Under certain conditions of pressure, temperature, and confinement time, alpha heating initiates a burn wave in the surrounding dense shell, leading to fusion energy outputs greatly exceeding the thermal and kinetic energy supplied to the DT fuel by the implosion [2]. Alpha heating is essential for ignition and energy gain in nuclear fusion.

In this Rapid Communication we show that recent direct drive OMEGA implosions [3] have achieved core conditions that would lead to significant levels of alpha heating if reproduced at scales typical of the National Ignition Facility (NIF) [4]. At NIF scale, these direct drive targets would yield about 125 kJ of fusion energy, 5× the highest fusion output achieved to date in ICF. The level of alpha heating and yield amplification is predicted to be similar to that achieved with the 1.9 MJ indirect-drive NIF [4] high foot (HF) implosions [5]. These HF implosions have achieved record fusion yields of nearly 10^{16} neutrons or about 26 kJ of fusion energy [6], demonstrating significant levels of alpha heating. Based on analytic models and detailed numerical simulations [7,8], it was estimated that alpha-particle heating has led to a ∼2–2.5× enhancement of the fusion yield [6,8]. In the absence of alpha heating, the fusion yield from hydrodynamic compression alone would have been ∼$4–5\times10^{15}$. By extrapolating recent OMEGA results in size to match the 1.9 MJ of incident NIF laser energy, we find that the best-performing direct-drive OMEGA implosion to date would lead to a neutron yield of 4.5×10^{16} neutrons and a level of alpha heating corresponding to about a 2× yield enhancement, similar to the indirect-drive HF targets at the same laser energy. The larger fusion yield in direct drive, results from the larger size and fuel mass of the 1.9 MJ direct-drive targets. A burning plasma metric [8], Q_α = alpha energy/pdV work > 1 determines the burning-plasma regime, where the energetics is dominated by the alpha heating. In this Rapid Communication a $Q_\alpha \approx 0.5$ is inferred for OMEGA implosions extrapolated to 1.9 MJ.

In order to evaluate the performance of implosions obtained with drivers of limited energy, an approach has been developed to extrapolate fusion yields, including alpha heating from current direct-drive inertial confinement fusion experiments on OMEGA at tens of kilojoules of incident laser energy to multi-megajoule drivers. The results of the extrapolation are first obtained analytically and then validated by multi-dimensional simulations. The analytic theory uses the three-dimensional hydro-equivalent scaling developed by Nora *et al.* [9] and Bose *et al.* [10]. These theories do not include the effect of alpha heating and can only be applied to extrapolate fusion yields and hydrodynamic properties due to compression alone without accounting for alpha-energy deposition (i.e., "no-alpha" properties). The effect of alpha heating is included separately using the model of Betti *et al.* [8], where the fusion-yield enhancement by alphas is estimated using the no-alpha properties of the implosion. The analytic results are validated with numerical simulations. We first directly simulate the OMEGA implosions using radiation–hydrodynamic codes and reproduce the core conditions to match all of the experimental observables. The simulation is then scaled hydroequivalently to larger sizes and laser energies to determine the fusion yield and the level of alpha heating. We find that the predictions of the analytic model are in good agreement with the results of direct simulations.

The scaling assumes that an implosion on a smaller laser facility is duplicated on a larger laser to reproduce the same energy density (i.e., pressure) but over a larger volume surrounded by a compressed cold shell of the same density and shape. The laser intensity is kept constant while the target mass and volume scale with the absorbed laser energy; therefore, implosion velocity and in-flight adiabat are the same, leading to an equivalent acceleration history. This implies that the implosions are hydrodynamically identical with a larger target dimension and time scale $R \sim t \sim E_{\mathrm{L}}^{1/3}$, where E_{L} is the laser energy. It follows that the linear and nonlinear growth factors of the hydrodynamic instabilities are equivalent [9,10]. The three-dimensional hydroequivalent scaling assumes that all the initial nonuniformities scale with target size, leading to the same level of shell distortion.

With regard to laser plasma instabilities and interactions (LPIs) in the coronal plasma, this Rapid Communication does not attempt to predict their scaling with size and energy. It is well known that LPIs do not scale proportionally with size and it is not possible to quantitatively extrapolate the effects of LPI at NIF energies from OMEGA results. LPI experiments at ignition scale energies on the NIF will be conducted over the next several years to determine laser-target coupling and the effects of LPIs. The goal of these studies is to demonstrate coupling similar to or improved over that observed on OMEGA. For the purpose of this Rapid Communication, we assume that LPIs on NIF will allow one to reproduce the same OMEGA implosion (equal velocity and adiabat) at the larger scale to match the 1.9 MJ NIF energy.

It is important to emphasize that predicting performance on different laser systems (OMEGA and NIF) is not the purpose of this Rapid Communication. The accuracy of such an extrapolation depends on the ability to correctly simulate current and future experiments, and to correctly capture all the sources of degradation [11] of implosion performance from low- to high-mode asymmetries, from nonlocal electron transport to laser plasma coupling. The goal of this Rapid Communication is much less ambitious but much more robust since it only assumes that the core conditions of an OMEGA implosion can be identically reproduced (same pressure, shell density, and shape) but with a larger spatial size on a larger laser facility. Therefore, in terms of hydrodynamic performance, the implosions at 1.9 MJ are assumed to be identical to the OMEGA implosions, just larger in target size by a factor of $(E_{\mathrm{NIF}}/E_{\mathrm{OMEGA}})^{1/3} \approx 4\times$. The only improvements brought by the larger size are in the thermal transport within the hot spot and the effect of alpha-particle energy deposition (or alpha heating). Both effects are based on straightforward physics considerations. Assuming the validity of Spitzer thermal conduction [12], the thermal transport improves at larger sizes (reduced surface/volume), leading to a modest increase in the central temperature. This can be determined by equating the rate of change of the hot-spot mass to the mass ablation rate off the shell inner surface into the hot spot. Mass ablation is driven by the heat flux leaving the hot spot and deposited on the shell inner surface,

$$\frac{dM}{dt} = S\dot{m}_{\mathrm{abl}}, \tag{1}$$

where M is the hot-spot mass, S is the hot-spot surface, and $\dot{m}_{\mathrm{abl}}$ is the mass ablation rate off the shell inner surface. We relate volume and surface to the linear dimension R ($S \sim R^2$, $V \sim R^3$). Using the ideal gas equation of state for the hot-spot plasma $\rho \sim P/T$, the hot-spot mass is $M \sim PV/T$, where P and T are hot-spot pressure and temperature. The mass ablation rate caused by the heat conduction from the hot spot is calculated by integrating the energy equation across the hot-spot boundary as in Ref. [10], yielding $\dot{m}_{\mathrm{abl}} \sim T^{5/2}/R$. During the final stage of the implosion (deceleration phase) the shell reaches peak implosion velocity and decelerates because of the increasing hot-spot pressure. The hydrodynamic time scale is $\tau \sim R/V_{\mathrm{imp}}$, where V_{imp} is the implosion velocity. Substituting these scaling relations into Eq. (1) leads to $T^{7/2} \sim PRV_{\mathrm{imp}}$. Since the hot-spot pressure and V_{imp} are unchanged in the hydrodynamic scaling, the temperature dependence with target size or laser energy follows $T \sim R^{2/7} \sim E_{\mathrm{L}}^{2/21}$ which is in fairly good agreement with the results of numerical simulations [13] showing $T \sim E_{\mathrm{L}}^{0.07}$. The difference in power indices (2/21 versus 0.07) is because of the effect of radiation losses on the temperature. The bremsstrahlung losses relative to the input pdV work increases with target size (at the relatively low areal densities of interest to laser fusion), reducing the benefits of the Spitzer temperature scaling. The $T \sim E_{\mathrm{L}}^{0.07}$ scaling includes the effects of the increased laser energy absorption occurring at a larger scale. In ideal hydroequivalent implosions, the absorbed fraction is assumed constant and we find that the power index is slightly smaller $T \sim E_{\mathrm{L}}^{0.06}$. This result indicates that hydrodynamically scaling the same implosion from OMEGA to NIF laser energy leads to a temperature increase of about 30% (but same pressure). The higher temperatures ($T \sim E_{\mathrm{L}}^{0.06} \sim R^{0.18}$), larger volumes ($V \sim R^3 \sim E_{\mathrm{L}}$), and longer confinement times ($\tau \sim R \sim E_{\mathrm{L}}^{1/3}$) in larger targets increase the fusion yield. The yield scales as $Y \sim n^2 \langle \sigma v \rangle V\tau$, where n is the DT particle density, $\langle \sigma v \rangle$ is the fusion reactivity, V is the burn volume, and τ is the confinement time. For yield amplifications less than ~ 10, most of the yield comes from the central hot spot and therefore the quantities above are related exclusively to the core. Using the fit for $\langle \sigma v \rangle / T^2 \sim T^{1.7}$ [14] leads to $Y \sim P^2 T^{1.7} V\tau$. Without accounting for alpha-energy deposition (no-α), the yield due to compression alone is obtained by substituting the size dependence of T, V, τ, and $P \sim$ const leading to the following scaling:

$$Y_{\text{no-}\alpha} \sim R^{4.3} \sim E_{\mathrm{L}}^{1.43}. \tag{2}$$

Equation (2) indicates that the compression yield increases by about 460× when extrapolating from a 26 kJ to a 1.9 MJ laser driver.

Estimating the level of alpha heating requires extrapolating the so-called no-α Lawson parameter $\chi_{\text{no-}\alpha}$. Following Ref. [8], $\chi_{\text{no-}\alpha}$ determines the yield enhancement caused by alpha heating by using exclusively no-α properties. There are different ways of expressing $\chi_{\text{no-}\alpha}$. Here we use the expression of Refs. [8,14,15] that is also related to the Livermore experimental ignition threshold factor (ITFx) [7,16,17]:

$$\chi_{\text{no-}\alpha} \approx (\rho R_{\text{no-}\alpha})^{0.61} \left(0.12 Y_{\text{no-}\alpha}^{16} / M_{\mathrm{DT}}^{\mathrm{stag}}\right)^{0.34}, \tag{3}$$

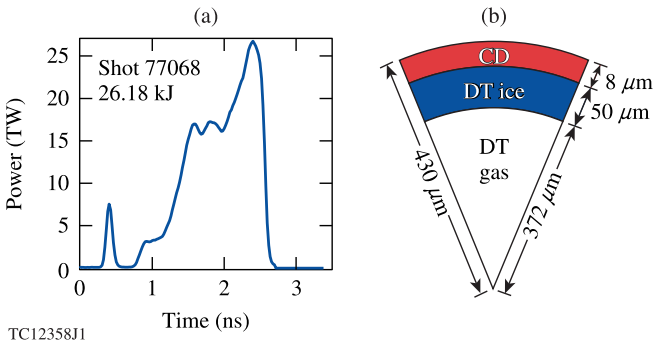

FIG. 1. OMEGA cryogenic implosion 77068: (a) laser power versus time (b) and target design.

TABLE I. Comparison of measurements with LILAC and DEC2D simulations (sim).

Observables[a]	Experiment [3]	1D sim.[b]	2D sim.[c]
Yield	$5.3\times10^{13}(\pm5\%)$	1.7×10^{14}	5.3×10^{13}
P^* (Gbar)	56(±7)	97	57
T_{ion} (keV)	3.6(±0.3)	3.82	3.7
R_{hs} (μm)	22(±1)	22	22
τ (ps)	66(±10)	61	54
ρR (g/cm^2)	0.194(±0.018)	0.211	0.194

[a]At 26.18 kJ laser energy.
[b]Using LILAC and DEC2D.
[c]Using DEC2D.

where ρR is in g/cm^2, the no-α neutron yield is in 10^{16}, and the stagnating DT mass at bang time is in milligrams. The latter is often approximated with 1/2 of the unablated DT mass [8,15] but in this Rapid Communication we use the more-accurate value from the simulation. Note that Eq. (3) is approximately equal to ITFx$^{0.34}$. Using the size dependence $\rho R_{\text{no-}\alpha} \sim R$, $M_{DT} \sim R^3$, and $Y_{\text{no-}\alpha} \sim R^{4.3}$ from Eq. (2) leads to the following hydrodynamic scaling of the no-α Lawson parameter:

$$\chi_{\text{no-}\alpha} \sim R^{1.05} \sim E_L^{0.35}. \tag{4}$$

The yield enhancement caused by alphas can be readily estimated once the $\chi_{\text{no-}\alpha}$ is determined. Using the fitting formula of Ref. [8], the fusion yield including alpha heating and the yield amplification are given by

$$Y_\alpha = \hat{Y}_{\text{amp}} Y_{\text{no-}\alpha}, \quad \hat{Y}_{\text{amp}} \simeq (1 - \chi_{\text{no-}\alpha}/0.96)^{-0.75}. \tag{5}$$

This analysis is applied to shot 77068, representative of the best-performing implosion on OMEGA to date [3]. Shot 77068 used a two-shock [18] 26.2 kJ single-picket laser-pulse with relaxation-type adiabat shaping [19]. The laser pulse shape and target design for this cryogenic implosion are shown in Fig. 1. The primary neutron yield measured by the 15.8 m neutron time-of-flight [20] detector was 5.0×10^{13} (±5%). Including the downscattered neutrons the total neutron yield becomes 5.3×10^{13}. The neutron-averaged areal density measured by the magnetic recoil spectrometer [21] was 0.194 (±0.018) g/cm^2. The initial DT mass of 27 μg was partially ablated; using one-dimensional (1D) radiation-hydrodynamic simulations, we estimate that about 18 μg remained unablated and about 11.5 μg is stagnating at bang time. All the relevant measurements and 1D simulation results are shown in the second and third columns of Table I. Applying the scaling in Eq. (2) from 26.2 kJ to 1.9 MJ of laser energy, we estimate that OMEGA implosion 77068 extrapolated to 1.9 MJ would produce 2.4×10^{16} neutrons from compression alone. To estimate the enhancement caused by alpha heating, we calculate the Lawson parameter for shot 77068. Using the measured areal density, neutron yield, and estimated stagnation mass, we find $\chi_{\text{no-}\alpha}(77068) \approx 0.138$ and its extrapolation [Eq. (4)] to 1.9 MJ is 0.61, which is close to the value of 0.66 estimated for the HF target [8]. The yield enhancement caused by alpha heating from Eq. (5) leads to an amplification of 2.1× and to a total neutron yield including alpha heating of about 5×10^{16} or 140 kJ of fusion energy. Note that the accurate power indices and parameters in the scaling laws are critically important for large extrapolations in energy. Indeed the power indices 1.5 and 0.37 in Ref. [9] [instead of 1.43 and 0.35 in Eqs. (2) and (4)] and the use of 1/2 DT mass instead of stagnating mass as in Eq. (3) would have lead to an extrapolated fusion yield of 270 kJ, ∼2× above the correct value.

We validated this new analytic scaling using direct simulations and reconstruction of all experimental observables. The OMEGA implosion is first simulated in 1D using the code LILAC [22]. This simulation indicates that the experiments are degraded with respect to 1D predictions (see Table I). The simulated 1D yield is 1.7×10^{14}, about 3.2× larger than measured. Simulated ion temperature, areal density, and burn duration are slightly above the measured value. Simulated and measured hot-spot sizes are the same and the experimentally inferred pressure [23] of 56 Gbar is below the 1D simulated value of 97 Gbar. To match the experimental observables, the implosion performance was degraded by adding a spectrum of target nonuniformities at the beginning of the deceleration phase. The radiation-hydrodynamic code DEC2D [10,24] was used to simulate the deceleration phase of the implosion starting from the 1D profiles from LILAC at the end of the laser pulse. In DEC2D, nonuniformities are introduced through angular perturbations of the velocity field on the inner surface of the shell (similar to Ref. [25]) that is Rayleigh-Taylor unstable during the shell deceleration. The

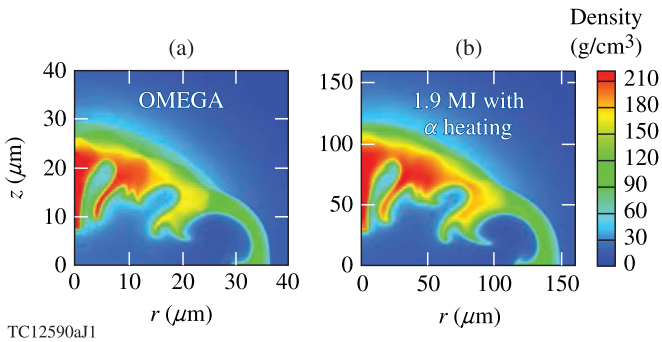

FIG. 2. Density contour plots from DEC2D at time of peak neutron rate for OMEGA shot 77068 (a) and hydroequivalent 1.9 MJ direct-drive implosion with alpha-particle energy deposition (b).

TABLE II. DEC2D simulation of OMEGA target and its hydroequivalent extrapolation to 1.9 MJ.

	OMEGA	1.9 MJ no-α	1.9 MJ with α
Yield	5.3×10^{13}	2.25×10^{16}	4.45×10^{16}
P^* (Gbar)	57	57	79
$T_{\rm ion}$ (keV)	3.7	4.7	5.1
$R_{\rm hs}$ (μm)	22	92.3	92.5
τ (ps)	54	215	193
ρR (g/cm^2)	0.194	0.83	0.81

spectrum of nonuniformities was chosen to reproduce the measured pressure, hot-spot radius (volume), and shape. Since long wavelength modes cause a reduction in hot-spot pressure, a dominant $\ell = 2$ mode was used with an amplitude 5% of the implosion velocity. To compensate for the increase in hot-spot volume caused by the $\ell = 2$ mode, a spectrum of intermediate mode numbers ($\ell = 4$–20) with amplitude 2% and high $\ell > 20$ modes with amplitudes $\sim 1/\ell^2$ was added. The mass density of the distorted OMEGA implosion at time of peak neutron rate is shown in Fig. 2(a); the hot-spot and dense fuel exhibit large distortions in shape. The results of two-dimensional (2D) simulations are shown in Table II indicating a fairly close match with the experimental observables. Figure 3 shows good agreement between the measured and simulated hot-spot shape [Figs. 3(a) and 3(b)] and emission profiles [Fig. 3(c)] from the time integrated x-ray images [26].

Using DEC2D, the simulation was scaled in size by 4.17× following the scaling $R \sim E_{\rm L}^{1/3}$ from 26.2 kJ to 1.9 MJ and keeping identical radial velocity, density, and temperature profiles. The same velocity perturbation was used to degrade the scaled implosion. The simulation was first performed without alpha-energy deposition. As expected (from Ref. [10]), the shape is almost identical; the only difference is the size. The core properties are listed in Table II and are consistent with the analytic scaling. The pressures are identical, whereas hot-spot radius, burn widths, and ρR scale by ∼4×. The hot-spot temperature is ∼30% higher for the larger implosion and the compression neutron yield increased by 425× to 2.25×10^{16}, similar to the analytic prediction. The DEC2D run was then repeated with the alpha-particle energy deposition turned on. The core conditions are shown in Fig. 2(b) and Table II. Including alpha-energy deposition produces a yield amplification of ∼2×, leading to a neutron yield of 4.45×10^{16} (125 kJ of fusion energy)— slightly below the analytic prediction. A burning plasma parameter $Q_\alpha \approx 0.5$ is inferred from $\hat{Y}_{\rm amp} \approx 2$ and Fig. 3 in Ref. [8].

Although it was possible to reproduce OMEGA experimental observables using the above spectrum of nonuniformities, the actual causes of degradation are currently uncertain.

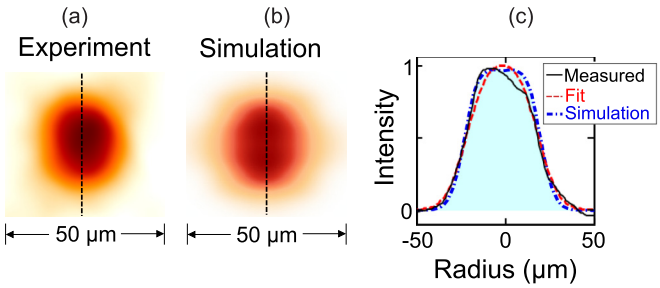

FIG. 3. Time integrated x-ray images of the hot spot from (a) experiment and (b) reconstructed from simulation; (c) comparison of intensity profiles along dashed line.

However, as mentioned above, the results of the extrapolation are independent of the degradation mechanism affecting OMEGA implosions. For example, we recover similar results if the 1D simulation of OMEGA shot 77068 is degraded by reducing the implosion velocity rather than by imposing 2D perturbations. Regardless of the degradation mechanism, the hydrodynamic extrapolation to a 1.9 MJ driver should lead to an approximately unique value of the fusion yield since the alpha heating depends primarily on the no-α Lawson parameter.

In conclusion, we have shown that 26 kJ direct-drive OMEGA implosions [3] have achieved core conditions (pressure, temperature, and density) that lead to significant alpha heating if hydrodynamically scaled to NIF energies. The predicted level of alpha heating leads to the doubling of the fusion output like in indirect-drive HF implosions on NIF. Fusion yields of ∼125 kJ are predicted, ∼5× that of the indirect-drive HF targets because of the larger mass of direct-drive targets. The importance of this Rapid Communication is that it shifts the emphasis for a successful NIF direct-drive implosion from hydrodynamics to laser-plasma interaction physics at the megajoule scale. This is because the hydrodynamics can be validated by scaling from OMEGA results (as done here). This Rapid Communicaton shows that if one can reproduce the same hydrodynamics of OMEGA targets on the NIF, then significant alpha heating is achievable. Therefore the emphasis in direct-drive ICF research should be in making sure that the LPIs on NIF do not degrade the implosion performance more than on the OMEGA targets.

The authors thank D. Shvarts for many useful discussions. This work has been supported by the U.S. Department of Energy under Cooperative Agreements DE-FC02-04ER54789 (Office of Fusion Energy Sciences) and DE-NA0001944 (National Nuclear Security Administration), and by the NY-SERDA.

[1] J. H. Nuckolls, L. Wood, A. Thiessen, and G. B. Zimmermann, Nature (London) **239**, 139 (1972).

[2] S. Atzeni and J. Meyer-ter-Vehn, *The Physics of Inertial Fusion* (Clarendon, Oxford, 2004); J. D. Lindl, *Inertial Confinement Fusion* (Springer, New York, 1998).

[3] S. P. Regan, V. N. Goncharov, I. V. Igumenshchev, T. C. Sangster, R. Betti, A. Bose, T. R. Boehly, M. J. Bonino, E. M. Campbell, D. Cao *et al.*, Phys. Rev. Lett. **117**, 025001 (2016).

[4] E. M. Campbell and W. J. Hogan, Plasma Phys. Control. Fusion **41**, B39 (1999); E. I. Moses, J. Phys.: Conf. Ser. **112**, 012003 (2008).

[5] O. A. Hurricane, D. A. Callahan, D. T. Casey, P. M. Celliers, C. Cerjan, E. L. Dewald, T. R. Dittrich, T. Döppner, D. E. Hinkel, L. F. B. Hopkins *et al.*, Nature (London) **506**, 343 (2014).

[6] T. Döppner, D. A. Callahan, O. A. Hurricane, D. E. Hinkel, T. Ma, H.-S. Park, L. F. Berzak Hopkins, D. T. Casey, P. Celliers, E. L. Dewald *et al.*, Phys. Rev. Lett. **115**, 055001 (2015); O. A. Hurricane, D. A. Callahan, D. T. Casey, E. L. Dewald, T. R. Dittrich, T. Döppner, M. A. Barrios-Garcia, D. E. Hinkel, L. F. Berzak Hopkins, P. Kervin *et al.*, Lawrence Livermore National Laboratory Report No. LLNL-JRNL-648209 (Appendix B), 2014 (unpublished).

[7] J. Lindl, O. Landen, J. Edwards, E. Moses, and NIC. Team, Phys. Plasmas **21**, 020501 (2014); **21**, 129902(E) (2014).

[8] R. Betti, A. R. Christopherson, B. K. Spears, R. Nora, A. Bose, J. Howard, K. M. Woo, M. J. Edwards, and J. Sanz, Phys. Rev. Lett. **114**, 255003 (2015).

[9] R. Nora, R. Betti, K. S. Anderson, A. Shvydky, A. Bose, K. M. Woo, A. R. Christopherson, J. A. Marozas, T. J. B. Collins, P. B. Radha *et al.*, Phys. Plasmas **21**, 056316 (2014).

[10] A. Bose, K. M. Woo, R. Nora, and R. Betti, Phys. Plasmas **22**, 072702 (2015).

[11] V. N. Goncharov, T. C. Sangster, R. Betti, T. R. Boehly, M. J. Bonino, T. J. B. Collins, R. S. Craxton, J. A. Delettrez, D. H. Edgell, R. Epstein *et al.*, Phys. Plasmas **21**, 056315 (2014).

[12] L. Spitzer, *Physics of Fully Ionized Gases* (Dover Publications, New York, 1956).

[13] C. D. Zhou and R. Betti, Phys. Plasmas **15**, 102707 (2008).

[14] R. Betti, P. Y. Chang, B. K. Spears, K. S. Anderson, J. Edwards, M. Fatenejad, J. D. Lindl, R. L. McCrory, R. Nora, and D. Shvarts, Phys. Plasmas **17**, 058102 (2010).

[15] P. Y. Chang, R. Betti, B. K. Spears, K. S. Anderson, J. Edwards, M. Fatenejad, J. D. Lindl, R. L. McCrory, R. Nora, and D. Shvarts, Phys. Rev. Lett. **104**, 135002 (2010).

[16] B. K. Spears, S. Glenzer, M. J. Edwards, S. Brandon, D. Clark, R. Town, C. Cerjan, R. Dylla-Spears, E. Mapoles, D. Munro *et al.*, Phys. Plasmas **19**, 056316 (2012).

[17] M. J. Edwards, P. K. Patel, J. D. Lindl, L. J. Atherton, S. H. Glenzer, S. W. Haan, J. D. Kilkenny, O. L. Landen, E. I. Moses, A. Nikroo *et al.*, Phys. Plasmas **20**, 070501 (2013).

[18] W. Theobald, R. Betti, C. Stoeckl, K. S. Anderson, J. A. Delettrez, V. Yu. Glebov, V. N. Goncharov, F. J. Marshall, D. N. Maywar, R. L. McCrory *et al.*, Phys. Plasmas **15**, 056306 (2008).

[19] K. Anderson and R. Betti, Phys. Plasmas **10**, 4448 (2003).

[20] V. Y. Glebov, D. D. Meyerhofer, C. Stoeckl, and J. D. Zuegel, Rev. Sci. Instrum. **72**, 824 (2001).

[21] J. A. Frenje, D. T. Casey, C. K. Li, J. R. Rygg, F. H. Sguin, R. D. Petrasso, V. Yu Glebov, D. D. Meyerhofer, T. C. Sangster, S. Hatchett *et al.*, Rev. Sci. Instrum. **79**, 10E502 (2008).

[22] J. Delettrez, R. Epstein, M. C. Richardson, P. A. Jaanimagi, and B. L. Henke, Phys. Rev. A **36**, 3926 (1987).

[23] C. Cerjan, P. T. Springer, and S. M. Sepke, Phys. Plasmas **20**, 056319 (2013).

[24] K. S. Anderson, R. Betti, and T. A. Gardiner, Bull. Am. Phys. Soc. **46**, 280 (2001); K. M. Woo, R. Betti, A. Bose, R. Epstein, J. A. Delettrez, K. S. Anderson, R. Yan, P.-Y. Chang, J. R. Davies, and M. Charissis, *ibid.* **59**, 354 (2015).

[25] R. Kishony and D. Shvarts, Phys. Plasmas **8**, 4925 (2001).

[26] F. J. Marshall and J. A. Oertel, Rev. Sci. Instrum. **68**, 735 (1997).